Measurement of sown area of winter wheat based on per-field classification and remote sensing imagery

GU Xiaohe[1], PAN Yaozhong[2], HE Xin[1], HUANG Wenjiang[1], ZHANG Jingcheng[1], WANG Huifang[1]

1. *National Engineering Research Center for Information Technology in Agriculture, Beijing* 100097, *China*;
2. *College of Resources Science & Technology, Beijing Normal University, Beijing* 100875, *China*

Abstract: With the significantly improved data availability in remote sensing technology, mid-resolution images have become the primary data source for crop sown area estimation in large scale. However, it is still difficult to solve the problems of spectrum heterogeneity in one field and spectra similarity between fields, especially in transitional region by using mid-resolution images. In order to maximally avoid above motioned problems and accurately measure the sown area of winter wheat, this paper developed per-field classification method and tested the method in an urban agriculture region with complex planting structure through several steps: first, digitalizing field boundary from QuickBird image; second, extracting characteristic index including spectrum and texture information as well as vegetation index for each field from the multi-temporal TM images; third, operating support vector machine (SVM) and maximum likelihood classification (MLC) with different field characteristic index; finally, estimating the accuracy of our method. Results show that the per-field classification method has a higher accuracy than per-pixel classification both in amount (estimated sown area of winter wheat divide by reference sown area of winter wheat, Kr) and position (equal to product accuracy, Kp). Although both SVM and MLC could get very high amount and position accuracy (97% and 90% respectively), the estimations of SVM are more stable. The errors of per-field classification mainly happened at the fragmentized parcels. Additionally, characteristic information could enhance the performance of per-field classification. Our method also has an outstanding advantage that no optimum period requires on satellite imagery which could enhance practicability and operationality of our method.

Key words: per-field classification, winter wheat, sown area, support vector machine, maximum likelihood

CLC number: TP79 **Document code:** A

Citation format: Gu X H, Pan Y Z, He X, Huang W J, Zhang J C and Wang H F. 2010. Measurement of sown area of winter wheat based on per-field classification and remote sensing imagery. *Journal of Remote Sensing.* **14**(4): 789—805

1 INTRODUCTION

The winter wheat is an important crop, whose sown area and yield are only lower than that of paddy in China. Accurate and real-time information of crop sown area is essential for yield estimation, agricultural management and national food security (Chen *et al*., 2005). The distinct character of the winter wheat distribution in China includes complex plant structure and fragmental planting parcel. Limitations on spatial resolution, availability and measurement accuracy of remote sensing images are the primary problems for sown area estimation of winter wheat in large-scale (Gu *et al*., 2007), which impedes the application of remote sensing on crop sown area investigation by official department.

Previous researches indicate that integration of multi-resolution images, in which mid-resolution images play the primary role, is the main trend to investigate crop sown area in large scale (Lobell *et al*., 2004; Van Niel *et al*., 2003; Langley *et al*., 2001). The per-pixel classifications developed on the statistical theory are the most popular methods used in crop information extraction from mid-resolution remote sensing image; however, they all face two common problems contributing on the reduction of classification accuracy (Smith & Fuller, 2001). First, the crop canopy reflectivity in farm parcels always occur spectra variation due to the influences of environmental humidity, nutrition, plant diseases and insect pests, which makes the same object with different spectra, causing omission errors. Second, mixed pixels on transitional region between different parcels may have similar spectral character and introduce commission errors. The lack of considering the context information is the crucial limitation of per-pixel based classification.

In order to solve the problems of spectrum heterogeneity in one field and spectra similarity between fields, many researches

Received: 2009-09-15; **Accepted**: 2010-01-29

Foundation: National Hi-Tech Research and Development Program of China (No. 2006AA120101, No. 2009AA12Z124) and the Beijing Excellent Talent Program (No. PYZZ090416001998).

First author biography: GU Xiaohe (1979—), male, Associate Scientist. He graduated from Beijing Normal University, and is now working for the study on agricultural application of remote sensing. He has published 13 papers. E-mail: guxh@nercita.org.cn

Corresponding author: PAN Yaozhong. E-mail: pyz@ires.cn

took the parcel as a basic unit and carried out the classification to minimize the shortage of per-pixel classification. The per-field classification divides remote sensing image into many basic units by the parcel boundary vector. For each parcel, the boundary of a parcel could provide the context information and label the inside pixels as the same land cover type. Previous studies have indicated that the accuracy of per-field classification is higher than that of traditional per-pixel classifications(Jassen *et al*., 1990; Pedley & Curran, 1991; Ban *et al*., 1995; Janssen & Molenaar, 1995; Lobo *et al*., 1996; Shandley *et al*., 1996; Aplin *et al*., 1999; Tso & Mather, 1999; Aplin & Atkinson, 2001, 2004; Smith & Fuller, 2001). Some relevant theories and application of per-field classification have been reported in China (Liu *et al*., 2000; Cheng *et al*., 2001; Wu *et al*., 2006), but the application of per-field classification on the estimation of crop sown area has not been paid so much attention so far.

Hence, in this paper we will test the performance of per-field classification on the estimation of crop sown area. An urban agriculture region with complex planting structure was chosen as study area and parcel boundaries were digitalized from QuickBird image. After that, we extracted characteristic index including the information of spectra, vegetation index and texture from multi-temporal TM images for each parcel, the classification unit and used support vector machine (SVM) and maximum likelihood classification (MLC) to distinguish winter wheat with different characteristic index or the composition of characteristic index. Finally, by using visual interpretation result from QuickBird image as the ground-truth, we validated the accuracy of our method and evaluated the performances of two classifiers coupled with different characteristic index or with their composition.

2 STUDY AREA AND MATERIALS

2.1 Study area

A typical urban agricultural region, Fangshan district in Beijing, was selected as the study domain where the majority crops are winter wheat, clover, corn, and soy bean. QuickBird images with extent of 100km^2 in Fangshan district, where the planting structure of winter wheat is similar to that in south China, were collected and used in this study.

The same crop has different spectra information in the remote sensing images during different phenological phases. The discrepancy among the different crop types at the same phenological stage can be used to select optimal period for crop area estimation. During November, the winter wheat was in the tillering stage, and the sown area of alfalfa was very small. From the middle April to the later May, the winter wheat grows well and its spectra information is easily distinct from other objects. Hence, the two periods were considered as the optimal phases for winter wheat detection in our study area.

2.2 Data preprocessing

A QuickBird image and multi-temporal TM images were adopted in this research (Fig.1). QuickBird image were collected on May 10, 2007, and TM images were acquired at December 3, 2006, April 26 and May 28, 2007, respectively. The QuickBird image was processed by merging pan band into multi-spectral bands and served as reference map for us to digitalize the parcel boundary and label the parcel land use type. The multi-temporal TM images served as the mid-resolution data source to provide characteristic vector. The preprocessing of remote sensing data included geometry correction, atmospheric correction and projection transformation.

Other auxiliary data included 1:10000 administrative boundary data, the distribution of cultivated land in Beijing in 2006, the statistical records of crop sown area from 2002 to 2006 and the field survey data in April 2007.

2.3 Preparation of farmland parcel database

The farmland parcel database is constructed by four steps: first, we established the classification system including winter wheat, fallow, woodland, grassland and vegetable land by analyzing the planting structure of the study area, field survey and land use data. Secondly, we manually digitalized the parcel boundary from QuickBird image as long as the area of the parcel was bigger than 0.25hm^2. Then we labeled land use type for each parcel by visual interpretation, which could be reviewed as ground-truth. Finally, we adopted a strict quality control criterion to check parcel boundary and labeled type, and complete the parcel database.

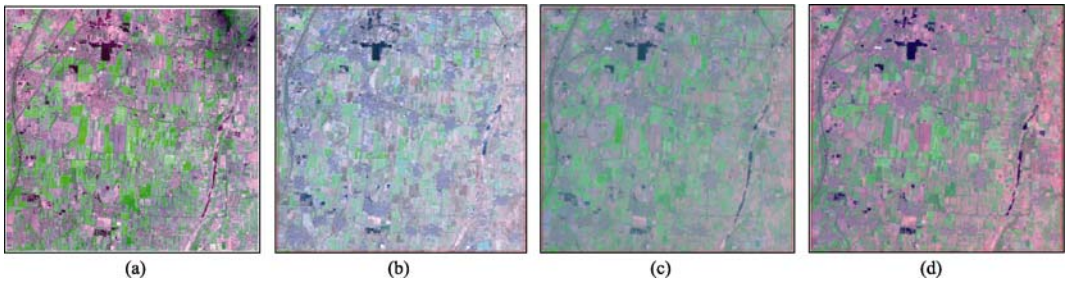

Fig. 1 QuickBird image and multi-temporal TM images in the study area
(a) 2007-05-10 QB image; (b) 2006-12-03 TM image; (c) 2007-04-26 TM image; (d) 2007-05-28 TM image

3 RESEARCH METHOD AND TECHNICAL PROCESS

Fig.2 shows our method used in this paper which includes calculating the coefficient of variation, selecting classifiers, combining characteristic index, calculating mean characteristic index for each parcel, choosing training samples, classifying through both per-field and per-pixel classification, and evaluating classification accuracy.

3.1 Construction of farmland parcel database

The boundaries of farmland parcels are stable in a long term, so they could be digitalized from former high-resolution images. In contrast, the crops type changes both seasonally and annually, and requires timely updated, which could be derived from the latest mid-resolution images. This paper just focuses on the pure parcel while the mixed parcel classification will be studied in the future by decomposition method. Hence, we firstly define the pure parcel with the assumption that if the land use type is homogenous (coefficient of variation (CV) < 0.1), the parcel is considered as pure parcel, otherwise as mixed parcel.

The function of coefficient of variation (CV) can be described as follows.

$$\mathrm{CV} = \frac{\sqrt{\frac{\sum (X_i - \bar{X})^2}{n}}}{\bar{X}} \tag{1}$$

Where $\bar{X}$ denotes the average value of the characteristic vector of all pixels in a parcel; n denotes the amount of pixels in a parcel; X_i denotes the characteristic vector value of one pixel in the parcel.

The CV indicates the scattering magnitude of the characteristic index of all pixels in one parcel. The mixed magnitude inside the parcel increases with CV increasing. Since the pure parcel also has a certain variance, the CV value could not reach zero. We calculated the parcel CV using all band of TM image for three temporal TM images, respectively. If all the CV values from three temporal TM images in one parcel are below 0.1, the parcel is regarded as a pure parcel, otherwise as a mixed parcel. Fig.3 shows the spatial distribution of pure parcels and mixed parcels.

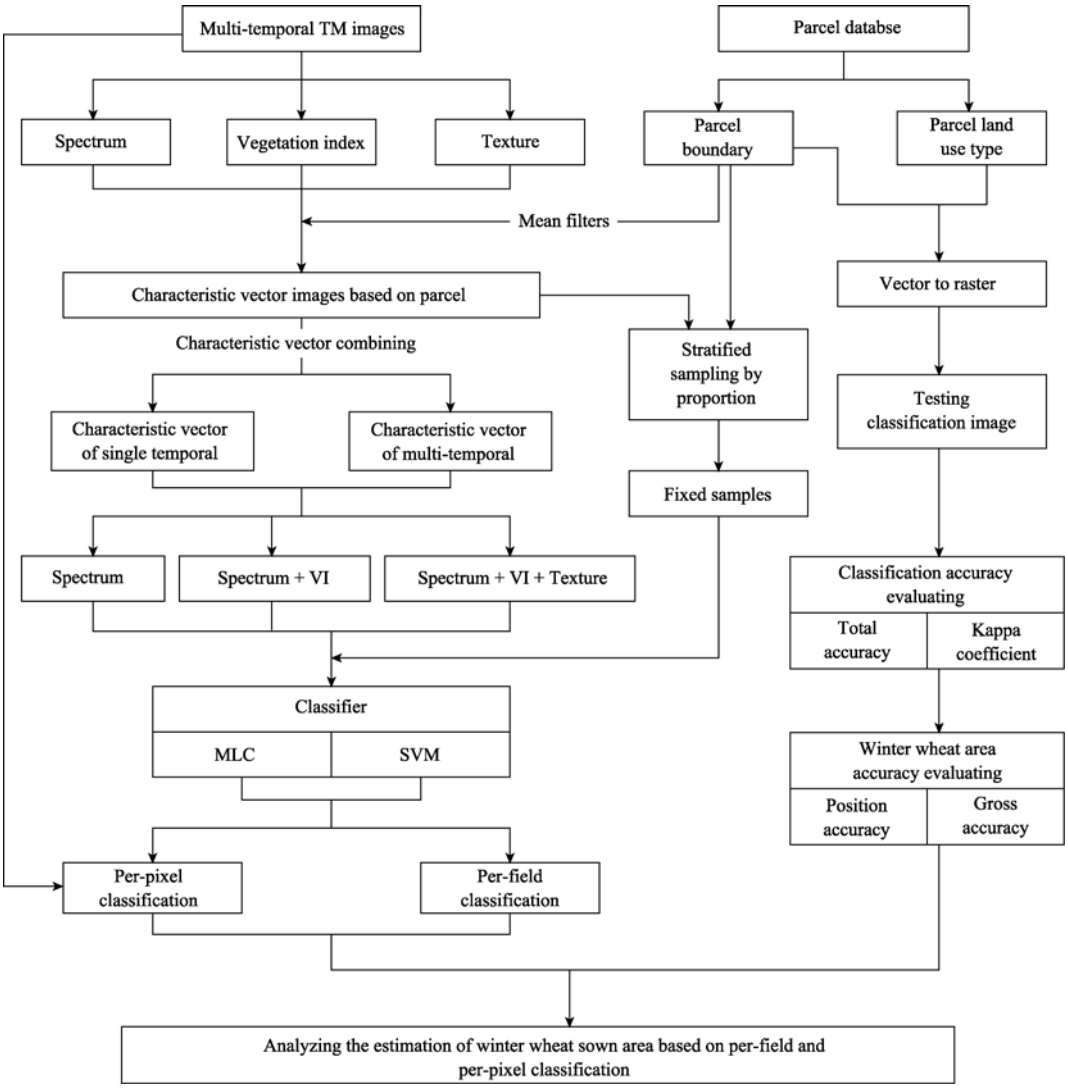

Fig. 2 Flow chart of technical process

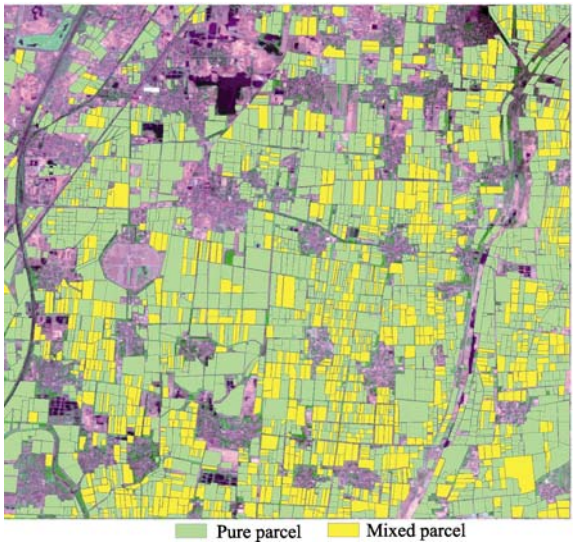

Fig. 3 Spatial distribution of pure parcel and mixed parcel

3.2 Selection of the classifier

The current classification methods of remote sensing were almost concentrated on using spectrum information, such as clustering criteria of spectrum distance, angle, probability, including neural network (Chen *et al*., 2007). The Maximum Likelihood Classification (MLC) based on parametric density distribution was the most commonly statistics method used in remote sensing supervised classification (Richards & Jia, 1999; El-Magd & Tanton, 2003). The Support Vector Machine (SVM) was widely used in image classification, target detection, data fusion etc. (He, 2007; He, 2006). In this study, we selected the MLC and the SVM as the typical classifiers for taking comparative analysis between per-field and per-pixel classification with different characteristic vectors combination.

3.3 Characteristic vector combination

In order to combine the application of the information of spectra, vegetation index and texture feature derived from multi-temporal TM images, three levels of vector combinations were designed (Table 1). The spectral feature vectors contained six bands of multi-temporal TM images. The vegetation index characteristic vectors included NDVI, RVI, SAVI, GVI, PVI and RDVI. The texture characteristic vectors covered variance, dissimilarity, entropy and correlation of the first component of TM image.

3.4 Calculation of the characteristic vector of parcel

We calculated the characteristic vector of a parcel by the following steps: first, calculating characteristic vectors from TM images for each pixel, including spectra reflectivity, vegetation index, and texture. Second, computing the mean characteristic vector of a given parcel based on Eq. (2). Third, assigning the mean characteristic vector to each pixel within the parcel.

$$F = \overline{X} = \frac{1}{n}\sum_{i=1}^{n} X_i \tag{2}$$

where $\overline{X}$ denotes the average value of a certain characteristic vector of all pixels in one parcel; n denotes the amount of pixels within the parcel; X_i denotes the characteristic vector value of one pixel in the parcel.

Table 1 Three levels of characteristic vector combinations of spectra, vegetation index and texture

Levels	ID	Combination way of characteristic vector
Spectra	a	Combination of 1—5,7 bands of TM image on Dec. 3rd, 2006
	b	Combination of 1—5,7 bands of TM image on Apr. 26th, 2007
	c	Combination of 1—5,7 band of TM image on May 28th, 2007
	d	Combination of 1—5,7 band of three temporal TM images
Spectra + VI	e	Combination of six bands and six VIs of TM image on Dec. 3rd, 2006
	f	Combination of six bands and six VIs of TM image on Apr. 26th, 2007
	g	Combination of six bands and six VIs of TM image on May 28th, 2007
	h	Combination of six bands and six VIs of three temporal TM images
Spectra + VI + Texture	i	Combination of six bands, six VIs and 4 textures of TM image on Dec. 3rd, 2006
	j	Combination of six bands, six VIs and 4 textures of TM image on Apr. 26th, 2007
	k	Combination of six bands, six VIs and 4 textures of TM image on May 28th, 2007
	l	Combination of TM image six bands, six VIs and 4 textures of three temporal TM images

3.5 Training samples selection

Considering the complex planting structure of our study area, it is crucial to choose optimum training samples both in quantity and quality for getting highly accurate classification results. Here, we adopted stratified proportion sampling method (Eq. (3)) to produce training samples from parcel database.

$$S = \sum_{i=1}^{n} N_i \times a\% \tag{3}$$

Where S denotes the amount of training samples; n denotes the amount of land use types; N_i denotes the total area of certain land use type parcel, which is provided by parcel database; a% denotes the sample proportion for each land use type.

To balance the computing efficiency and classification accuracy, we made the multiple tests and finally decided a 5% of sample proportion for MLC and a 1% of sample proportion for SVM because of good study ability of SVM for limited samples.

3.6 Method of result assessment

The accuracy assessment of classification is to evaluate the differences between classified result and reference map (or ground-truth). In this study, we used the visually interpreted results from QuickBird image as “ground-truth”, evaluated the accuracy for both per-field and per-pixel classification from multi-temporal TM images, and compared the classification accuracy from different classifiers and different feature vector combination by overall accuracy and Kappa coefficient derived from confusion matrix confusion matrix. We also estimated the measurement accuracy of sown area of winter wheat under different feature vector combination in two ways: amount accuracy and pixel accuracy (also called position accuracy).

(1) Position accuracy

The position accuracy is the ratio of correctly classified pixels/parcels to the total pixels/parcels in study area. For the per-field classification, the position accuracy is based on parcel units. As for per-pixel classification, the accuracy is based on pixel units. The formula of position accuracy is shown as follows.

$$K_p = \frac{\sum P_i \times A_i}{A_0} \times 100\% \quad (4)$$

where P_i denotes the number of correctly classified winter wheat parcels or pixels associated to a given feature vector combination; A_i denotes the acreage of correctly classified parcels or pixels of winter wheat; A_0 denotess the total acreage of all parcels of winter wheat from the parcel database.

(2) Amount accuracy

The amount accuracy of sown area of winter wheat is the ratio of estimated acreage to the true value in a given district or natural region (Eq. (5)).

$$K_r = 1 - \frac{|A_i - A_0|}{A_0} \times 100\% \quad (5)$$

where A_i denotes the estimated total acreage of winter wheat in the study region derived from per-parcel or per-pixel classification with certain characteristic vector combinations; A_0 denotes the total acreage of winter wheat from the parcel database.

4 RESULTS AND DISCUSSION

In this study, we extracted the training samples from high resolution parcel database by stratified random sampling and carried out both the per-field and per-pixel classification with twelve types of characteristic vector combinations and two classifiers (SVM and MLC). In order to reduce random errors and test the stability of classifiers, we carried out ten times classification for both SVM and MLC respectively, and each time with different training samples. The results are shown in Fig. 4. Furthermore, we used visual interpretation results from the QuickBird image as reference map, and evaluated our results from both position and amount perspectives (Fig.5 and Fig.6). Our results show:

(1) The per-field classification method has a higher accuracy

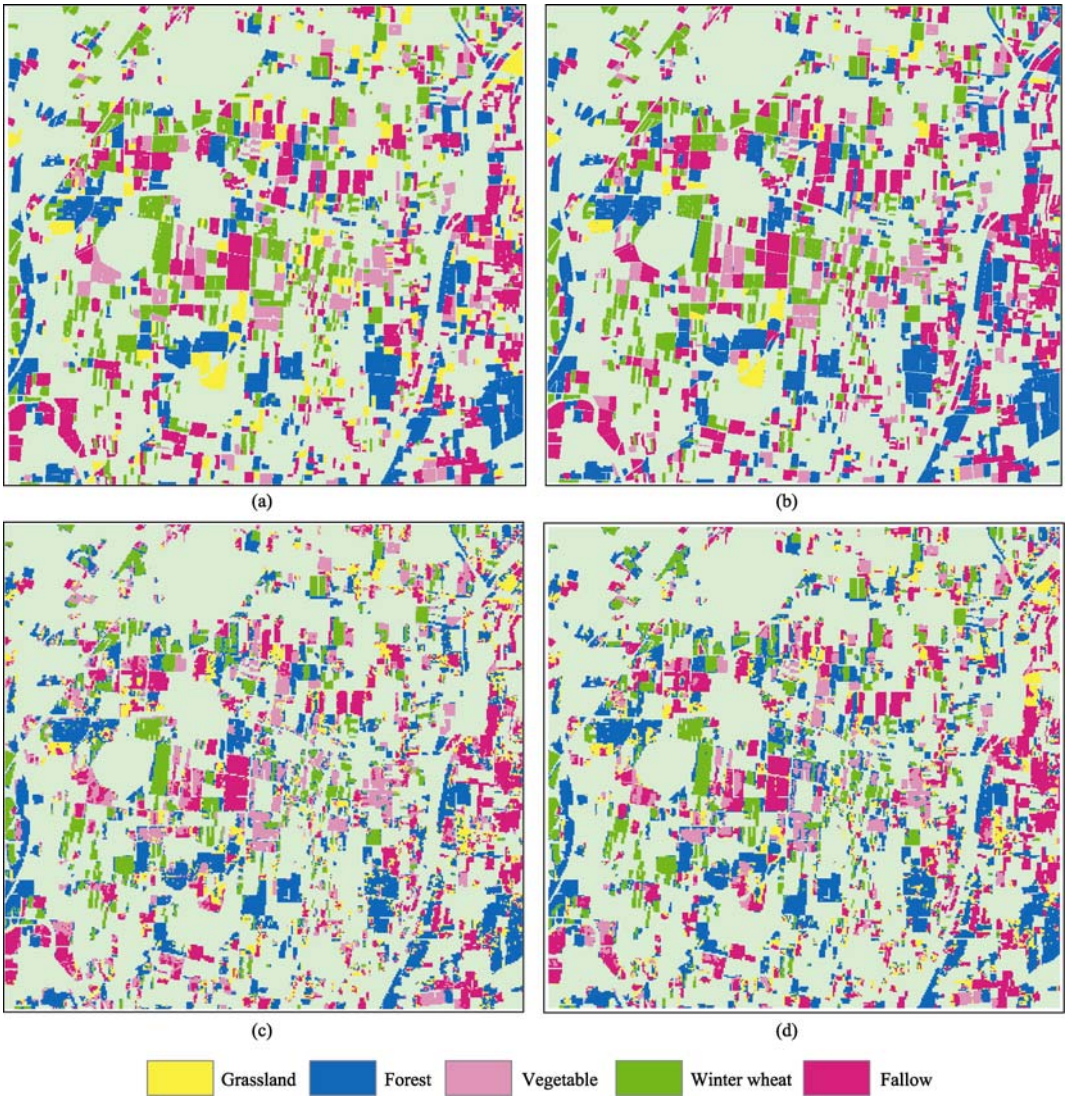

Fig. 4 Classified results from per-field and per-pixel using spectral, vegetation index and texture

(a) Per-field classification by MLC; (b) Per-field classification by SVM; (c) Per-pixel classification by MLC; (d) Per-pixel classification by SVM

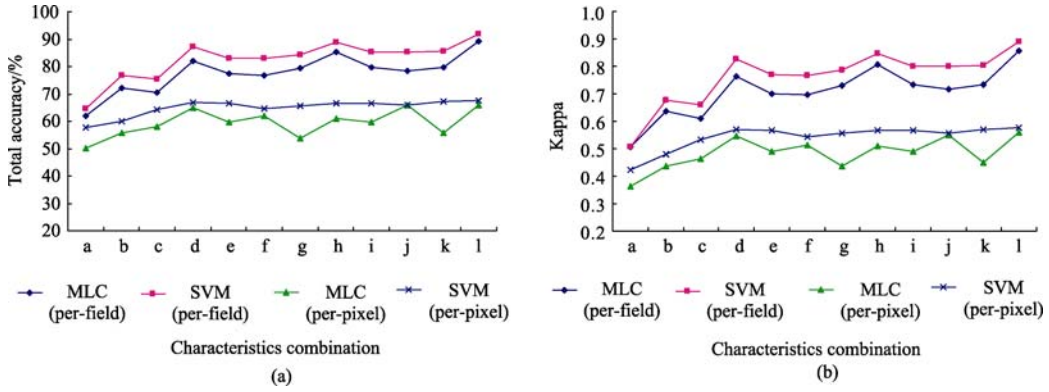

Fig. 5 Comparison of total accuracy and kappa coefficient between per-field and per-pixel classification by MLC and SVM algorithm
(The meaning of a—l is shown in Table 1.)
(a) Comparison of total accuracy between MLC and SVM algorithm in per-field and per-pixel classification; (b) Comparison of Kappa coefficient between MLC and SVM algorithm in per-field and per-pixel classification

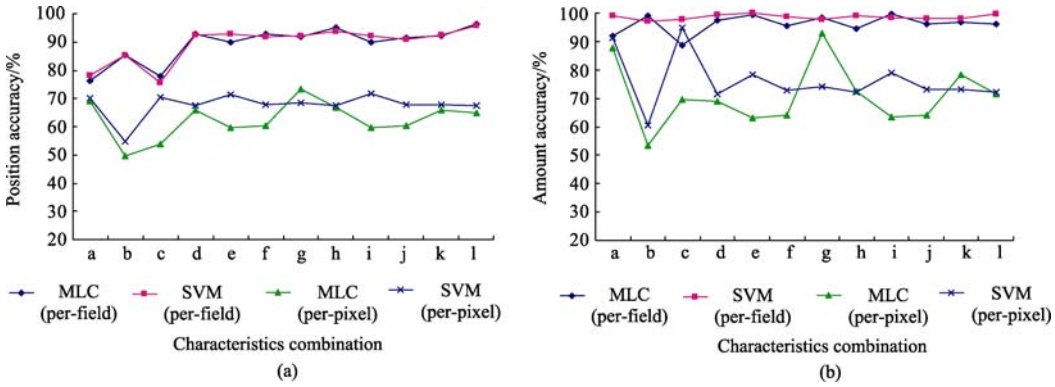

Fig. 6 Comparison of amount accuracy and position accuracy of winter wheat planting area between per-field and per-pixel classification by MLC and SVM algorithm
(The meaning of a—l is shown in Table 1.)
(a) Position accuracy; (b) Account accuracy

than per-pixel classification both in amount and position. The overall accuracy and Kappa coefficient of per-field classification was 10% and 0.1 higher than those of per-pixel classification for the most of characteristic vector combinations. The amount and position accuracy of per-field classification were 95% and 90% respectively, which means the per-field classification could reduce the commission. It also indicates that the omission and commission errors of per-field classification are far below than those of per-pixel classification in complex planting area. Hence, it is potential to use per-field classification to estimate the sown area of winter wheat in different regions.

(2) The overall accuracy and Kappa coefficient of per-field classification increased faster than those of per-pixel classification with the characteristic vector increasing which means the information of vegetation index and texture could improve the accuracy of per-field classification, but not the accuracy of per-pixel classification. However, for the winter wheat sown area estimation, the information of vegetation index and texture could only improve the position accuracy.

(3) The accuracy of per-field classification from multi-temporal images is higher than that of a single image, which indicates that the difference of crop phenology could improve the overall accuracy and Kappa coefficient. When the periods of TM images were increased, the amount accuracy of winter wheat kept stable but the position accuracy was improved gradually. That is to say the peculiar phenology of winter wheat does not improve the amount accuracy of sown area estimation of winter wheat but does improve the position accuracy in our study area. As for the per-field classification with a single image, the amount accuracy and position accuracy in jointing period are higher than that in overwintering and grain-filling period.

In order to analyze the error source in the per-field classification of winter wheat, we divided the winter wheat parcels into ten different intervals based on the parcel acreage, kept the number of parcel consistent in each interval, and then took the combination of three temporal spectra, vegetation index and texture with high accuracy as an example to analyze the spatial distribution of commission and omission errors by calculating the correct rate, commission rate and omission rate of winter wheat parcel within all kinds of intervals.

With the parcel area expanding, the correct rate of winter wheat parcel with per-field classification was improved, while the commission rate and omission rate were decreased (Fig. 7).

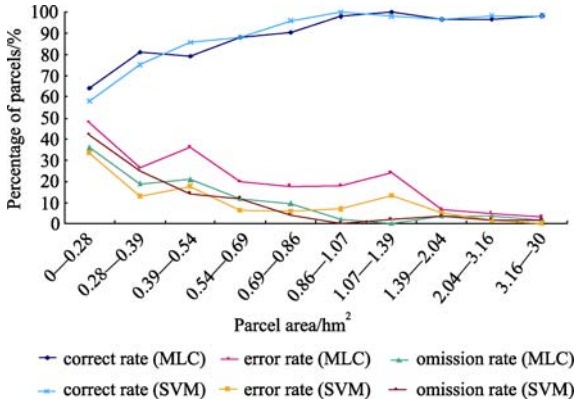

Fig. 7 Accuracy of winter wheat by per-field classification with different parcel area interval

It is because the spectra of fragmentized parcels were more likely to be mixed and difficult to distinguish, causing the commission errors. In contrast, the omission in large parcel tends to be lower. The error rate of winter wheat parcel by MLC was higher than by SVM. Since the better learning ability of the SVM algorithm, it had a lower omission rate of winter wheat parcels than MLC did when using the same size of samples. Hence, the SVM is more robust for per-field classification than MLC in sown area estimation of winter wheat.

The commission and omission of winter wheat based on per-field classification mostly happens in the fragmental parcels, but the acreage of fragmental parcels is very small. Therefore, the errors caused by fragmental parcels didn't influence the overall accuracy at all, and it is reasonable to conclude that the per-field classification could obtain higher accuracy in both amount and position than per-pixel classification in the whole study area. When conducting practical measurement, if a small quantity of commission and omission classification occurring in a large winter wheat parcels, we could modify them through field investigation with small workload.

5 CONCLUSION AND PERSPECTIVE

In order to estimate the sown area of winter wheat accurately, this paper took an urban agricultural zone with complex planting structure as study area, and carried out the comparative analysis between the per-field and per-pixel classifications based on multi-temporal TM images. Our results show that firstly the per-field classification method has a higher accuracy than per-pixel classification both in amount and position. Second, although both SVM and MLC could get very high amount and position accuracy (97% and 90%, respectively), the estimation of SVM is more stable and requires less training samples, which indicate the SVM is more robust for per-field classification than MLC in sown area estimation of winter wheat. Third, the information of vegetation index and texture improved the precision of per-field classification. Fourth, the estimation of winter wheat based on per-field classification has no limitation on the period of TM image. Howerve, it gets both higher amount and position accuracy in the jointing period of winter wheat. Finally, the errors of per-field classification mainly happen at the fragmentized parcels.

The basic idea of crop per-field classification is to segment the whole study area into small homogeneous classification unit (parcel) and label land use type based on classification unit instead of pixel, which makes spatial texture information involved into the process of classification, reducing omission errors caused by the problem of same object with different spectrum. Furthermore, the parcel boundary is stable for a long term, which could be easily digitized from previous high-resolution images. With the improvement of availability of high-resolution image as well as the expanding application of the second land use survey production, the boundary of farmland parcel is easier to obtain. The crops of farmland parcels vary year by year, so that we should define and update the land cover type for each parcel every year. Then, the current mid-resolution images could be a useful tool. For example, in this paper, considering the size of farmland parcels is much larger than the pixel size of mid-resolution image, we distinguished the pure parcel and mixed parcel by calculating the CV of pixels inside of each parcel, carried out the per-field classification for pure parcels, and got a high accuracy. Considering our study area is in urban agricultural region with fragmental planting parcel, the accuracy could be expected to improve in regions with simple planting structure or less fragmental parcels. To sum, our method has potential applicability to accurately estimate the sown area of winter wheat in different planting structure regions.

This study still needs to be improved in future. First, the paper carried out the per-field classification in 100km^2 region; we need to test our result in larger scale. Second, the separability of different land use types affects the classification accuracy. The land use type in our study included winter wheat, fallow land, forest, grassland and vegetable. The classification accuracy of vegetable and grassland is lower; moreover, both of them are easy to be confused with fallow land in December. If we find higher efficient classification algorithm in the future, the accuracy of per-field classification will be further improved.

REFERENCES

Aplin P, Atkinson P M and Curran P J. 1999. Fine spatial resolution simulated satellite sensor imagery for land cover mapping in the United Kingdom. *Remote Sensing of Environment*, **68**: 206—216

Banair A, Morin D, Bonn F and Huete A R. 1995. A review of vegetation Indices. *Remote Sens. Review*, **13**: 95—120

Chen C X, Yan T L and Zhu D H. 2001. The method of polygon land use identify supported by GIS. *Journal of China Agricultural University*, **6**(3): 55—59

Chen L, Liu X and Zhang Y. 2007. A study of image classification based on MLC combined with spectral angle. *Engineering of Surveying and Mapping*, **16**(3): 40—47

Chen S S, Liu Q H, Chen L F, Li J and Liu Q. 2005. Review of research advances in remote sensing monitoring of grain crop area. *Transactions of the Chinese Society of Agricultural Engineering*, **21**(6): 166—171

David B.Lobell and Gregory P.Asner. 2004. Cropland distribution from temporal unmixing of MODIS data. *Remote Sensing of Environment*. **93**: 412—422

Drezetp M L and Harrison R F. 2001. A new method for sparsity control in support vector classification and regression. *Pattern Recognition*, **34**: 1112—1125

El-Magd I A and Tanton T W. 2003. Improvements in land Use mapping for irrigated agriculture from satellite sensor data using a multi stage maximum likelihood classification. *International Journal of Remote Sensing*, **24**(21): 4197—4206

Gu X H, Pan Y Z, Zhu X F, Zhang J S, Han L J and Wang S. 2007. Consistency study between MODIS and TM on winter wheat plant area monitoring. *Journal of Remote Sensing*, **11**(3): 350—358

He D P, Xiao Y, Xiao X G, Huang Y H and Zhou Q R. 2006. Application of the support vector machine in remote sensed image processing. *Urban Geotechnical Investigation & Surveying*, **3**: 27—30

He L M, Shen Z Q, Kong F S and Liu Z K. 2007. Study on multi-source remote sensing images classification with SVM. *Journal of Image and Graphics*, **12**(4): 648—654

Janssen L L F, Jaarsma M N and Van der Linden E T M. 1990. Integration topographic data with remote sensing for land-cover classification. Photogrammetric Engineering and Remote Sensing, **56**: 1503—1506

Langley S K, Cheshire H M and Humes K S. 2001. A comparison of single date and multitemporal satellite image classification in a semi-arid grassland. *Journal of Arid Environments*, **49**: 401—411

Liu J G, Zhang B, Zheng L F and Tong Q X. 2000. Urban remote sensing application study using hyperspectal data. *Journal of Remote Sensing*, **4**(3): 224—227

Lobo A, Chic O and Casterad A. 1996. Classification of mediterranean crops with multisensor data: per-pixel versus per-object statistics and image segmentation. *International Journal of Remote Sensing*, **17**: 2385—2400

Pedley M I and Curran P J. 1991. Per-field classification: an example using SPOT-HRV imagery. *International Journal of Remote Sensing*, **12**: 2181—2192

Shandley J, Franklin J and White T. 1996. Testing the Woodcock-Harward image segmentation algorithm in an area of southern California chaparral and woodland vegetation. *International Journal of Remote Sensing*, **17**: 983—1004

Smith G M and Fuller R M. 2001. An integrated approach to land cover classification: an example in the Island of Jersey. *International Journal of Remote Sensing*, **22**: 3123—3142

Smith G M and Fuller R M. 2001. An integrated approach to land cover classification: an example in the Island of Jersey. *International Journal of Remote Sensing*, **22**: 3123—3142

Van Niel, T G. and McVicar, T R. 2003. A simple method to improve field-level rice identification: toward operational monitoring with satellite remote sensing. *Australian Journal of Experimental Agriculture*, **43**: 379—387

Wu J P, Mao Z H, Chen J Y and Pan D L. 2006. A new classification method for coast remote sensing image. *Journal of Martine Sciences*, **24**(2): 70—78

以地块分类为核心的冬小麦种植面积遥感估算

顾晓鹤[1]，潘耀忠[2]，何　馨[1]，黄文江[1]，张竞成[1]，王慧芳[1]

1. 国家农业信息化工程技术研究中心，北京 100097;
2. 北京师范大学 资源学院，北京 100875

摘　要：以提高冬小麦种植面积估算精度为目标，选取种植结构复杂的都市农业区，采用 QuickBird 影像数字化农田地块边界，以多时相 TM 影像为核心数据源，以地块为基本分类单元，进行不同特征向量组合、不同分类器的冬小麦地块分类方法研究，并对比分析了基于地块分类和基于像元分类的冬小麦种植面积估算精度。研究结果表明，基于地块分类的冬小麦种植面积估算方法的总量精度和位置精度均高于像元分类；植被指数和纹理信息的引入有助于进一步提高地块分类精度；支持向量机与最大似然均能得到高达 97%的总量精度和 90%的位置精度，支持向量机地块分类所需的训练样本量远低于最大似然，因此支持向量机更加适合于冬小麦地块分类；冬小麦错分与漏分情况大多发生在细碎地块，其面积总量较小，而大地块错分和漏分较少，因此相对于像元分类，地块分类能在整个区域能得到较高的冬小麦位置精度和总量精度。

关键词：地块分类，冬小麦，种植面积，支持向量机，最大似然

中图分类号：TP79　　文献标识码：A

引用格式：顾晓鹤，潘耀忠，何　馨，黄文江，张竞成，王慧芳. 2010. 以地块分类为核心的冬小麦种植面积遥感估算. 遥感学报, **14**(4): 789—805

Gu X H, Pan Y Z, He X, Huang W J, Zhang J C and Wang H F. 2010. Measurement of sown area of winter wheat based on per-field classification and remote sensing imagery. *Journal of Remote Sensing*. **14**(4): 789—805

1　引　言

冬小麦作为中国第二大粮食作物，其种植面积和产量仅次于水稻，是中国最重要的粮食作物之一。准确获取区域冬小麦种植面积信息及其空间分布状况，对于预测小麦产量，优化种植空间格局，确保国家粮食安全具有重要意义(陈水森, 2005)。中国冬小麦的显著空间特征是范围广、种植结构复杂、种植地块破碎，当前大范围冬小麦遥感估算存在的核心问题是遥感影像的空间分辨率、获取能力和测量精度之间相互制约的问题(顾晓鹤，2007)，导致遥感技术在冬小麦种植面积估算中的应用长期处于科学研究和准业务运行阶段。

大量研究工作(Lobell 等，2004; Van Niel 等，2003; Langley 等, 2001)表明，以中分辨率数据为主、低分辨率数据为辅的估算方法是大范围农作物种植面积估算的主要趋势之一。基于统计学理论的像元逐点分类是绝大多数计算机辅助下农作物遥感信息提取所采用的传统方法，经常用于中分辨率遥感影像的作物识别上，但始终存在两个常见的分类问题严重影响着作物像元分类精度(Smith & Fuller, 2001)。第一，农田中的作物冠层反射率常常由于环境湿度、生长状况、营养条件或者病虫害等因素的影响而产生光谱变异，使得同一作物种植块中出现某些像元的光谱特征与大部分像元相异，或同类型作物种植块内光谱变频高的“同物异谱”现象，致使在像元分类过程中将光谱变异的像元根据其光谱距离错判为其他类型。第二，两类不同作物的田块交界处由于相邻像元之间能量的传递作用存在较多的混合像元，往往会依其混合光谱值而被错分至其他作物类型。该两大问题大大降低了基于像元的作物分类的可靠性，其主要原因在于将各像元孤立开

收稿日期：2009-09-15；修订日期：2010-01-29

基金项目：国家高技术研究发展计划(编号: 2006AA120101 和编号: 2009AA12Z124)及北京市优秀人才计划(编号: PYZZ090416001998)。

第一作者简介：顾晓鹤(1979—)，男，博士，助理研究员，毕业于北京师范大学。现主要从事农业遥感应用研究，已发表论文 13 篇。E-mail: guxh@nercita.org.cn。

通讯作者：潘耀忠, E-mail: pyz@ires.cn。

来确定类型，丢失了像元之间可利用的上下文关系，极易产生“椒盐现象”。

针对像元分类所面临的地块内部光谱变异与地块边界光谱混合的问题，许多学者采取以地块为基本单元的分类方式来克服像元分类所遇到的问题，以提高遥感分类精度。地块分类的基本思想是以农田地块的边界将遥感影像分割成许多个基本地块单元，对每一地块，边界即是对地块内部像元之间上下文的定义，使得这些像元可以一并参与分类处理，这即是地块分类与像元分类的不同之处。大量研究表明(Jassen 等, 1990; Pedley & Curran, 1991; Ban 等, 1995; Janssen & Molenaar, 1995; Lobo 等, 1996; Shandley 等, 1996; Aplin 等, 1999; Tso & Mather, 1999; Aplin & Atkinson, 2001, 2004; Smith & Fuller, 2001)，面向地块的土地覆盖分类方法能够提供比基于像元的传统分类法更精确的结果。面向地块的遥感分类思想在中国也有一些相关的理论研究与应用。刘建贵等(2000)利用高空间分辨率图像检测出城市各地物的轮廓线，形成多边形地块，进行逐地块统计分析和分类，结果证明此方法很适合复杂的城市土地利用信息的提取。程昌秀等(2001)利用 GIS 地块边界信息，提出标准土地利用类型的地块边界内的灰度特征、纹理特征和形态特征，建立决策树分类方法，其识别准确率较高。吴均平等(2006)利用基于分割图斑的分类法对动态多变、混杂度大的海岸带进行分类，在一定程度上提高了分类精度，具有良好的抗噪性，但该方法在道路的分类上由于邻接地物复杂造成错分概率较高。总体来说，现有以地块为基本单元的分类方法研究在土地覆盖遥感信息提取方面获得了一定程度的发展，但尚没有将地块分类的优势系统化地应用于农作物种植面积信息提取方面。

估算精度是农作物种植面积遥感估算技术进入业务化运行阶段的必要前提。本文选取种植结构复杂的都市农业区为方法实验区，通过高分辨率 QuickBird 影像人工数字化的方式获取实验区地块边界，以地块为基本单元获取多时相 TM 影像特征信息，构建光谱、植被指数和纹理三层次特征向量组合方式，采取分层等比例方式选取训练样本，利用最大似然和支持向量机进行地块分类，并从影像分类精度和冬小麦种植面积估算精度两个方面进行地块级和像元级分类精度的对比分析，探索适用于种植结构复杂区域的冬小麦地块分类的特征向量组合和分类方法。

2 研究区及其数据

2.1 研究区概况

北京房山区属于典型都市农业区，种植的农作物主要有冬小麦、苜蓿、玉米、大豆等，虽然不是中国冬小麦的主产区，但分布着种植结构复杂的冬小麦，具有较好的典型性。本研究选取北京市房山区内的 100km^2 的 QuickBird 影像覆盖区作为实验区，该地区地块破碎度较高，与中国南方冬小麦种植特征相似，具有较好代表性。

由于同一作物在不同物候期的遥感图像上有不同的光谱特征，作物物候历的种间差异是选择作物识别时相的常用依据。11 月上旬至下旬，冬小麦处于分蘖期，而同期苜蓿种植面积很小；4 月中旬至 5 月下旬，冬小麦处于旺盛生长期，其光谱信息最显著，而春播作物刚刚播种，因此，可把这两段时期定为冬小麦识别较优时间段。

2.2 数据准备

本研究使用的遥感数据主要是 QuickBird 影像与多时相 TM 现势影像。其中 QuickBird 数据为多光谱和全色波段融合影像，成像时间为 2007 年 5 月 10 日，见图 1(a)，用于人工数字化地块边界，为 TM 影像地块分类提供边界信息和冬小麦种植面积“准真值”；多时相 TM 影像作为核心数据源为地块分类提

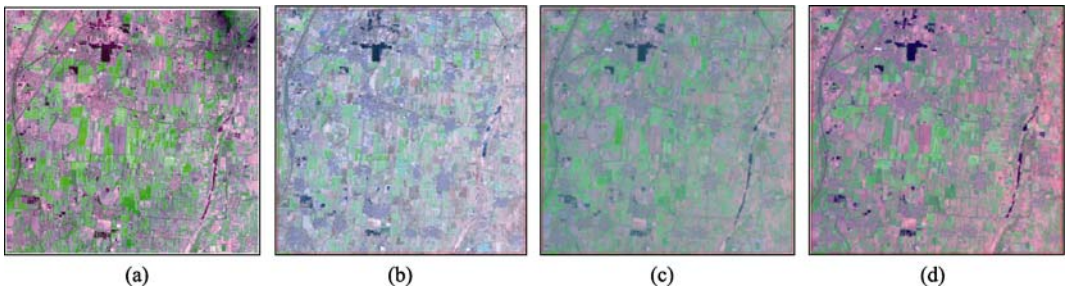

图 1 房山实验区 QuickBird 和多时相 TM 数据

(a) 2007-05-10 QB image; (b) 2006-12-03 TM image; (c) 2007-04-26 TM image; (d) 2007-05-28 TM image

供特征向量信息，时相分别为 2006-12-03、2007-04-26 和 2007-05-28，见图 1(b)—(d)。遥感数据预处理主要包括几何纠正、大气校正和投影变换等。

本研究于 2007 年 4 月 15-16 日开展野外调查，共获取 217 个野外观测样本地块，包括冬小麦、休耕地、林地、草地、菜地等类型，为高分辨率影像目视解译提供先验知识和样本信息。

此外，本研究采用的辅助数据还包括：2006 年北京耕地本底数据、1∶1 万北京市行政边界数据、2002—2006 年农作物统计数据、2007 年 4 月的野外调查数据。

2.3 地块数据库建设

采用 QuickBird 影像进行地块本底数据库建设的基本思路是：首先通过野外调查和土地利用数据进行实验区种植结构分析，建立包括冬小麦、休耕地、林地、草地、菜地在内的分类体系,建筑用地、河流、道路等不影响冬小麦识别的地类则采用目视解译的方式剔除，不参与地块分类方法研究；采用屏幕人工数字化方式，按照统一的标准规范对 QuickBird 影像进行地块边界数字化，地块最小面积为 0.25hm^2；采用目视解译的方式识别各种地物，统计实验区内冬小麦种植面积总量，作为地块分类方法研究的检验“准真值”。

3 研究方法与技术流程

基于地块分类的冬小麦种植面积遥感估算的技术流程如图 2，包括地块变异系数计算、分类器选取、特征向量组合、基于地块的特征向量提取、训练样本选取、地块分类、与像元分类对比分析和精度评价等主要流程。

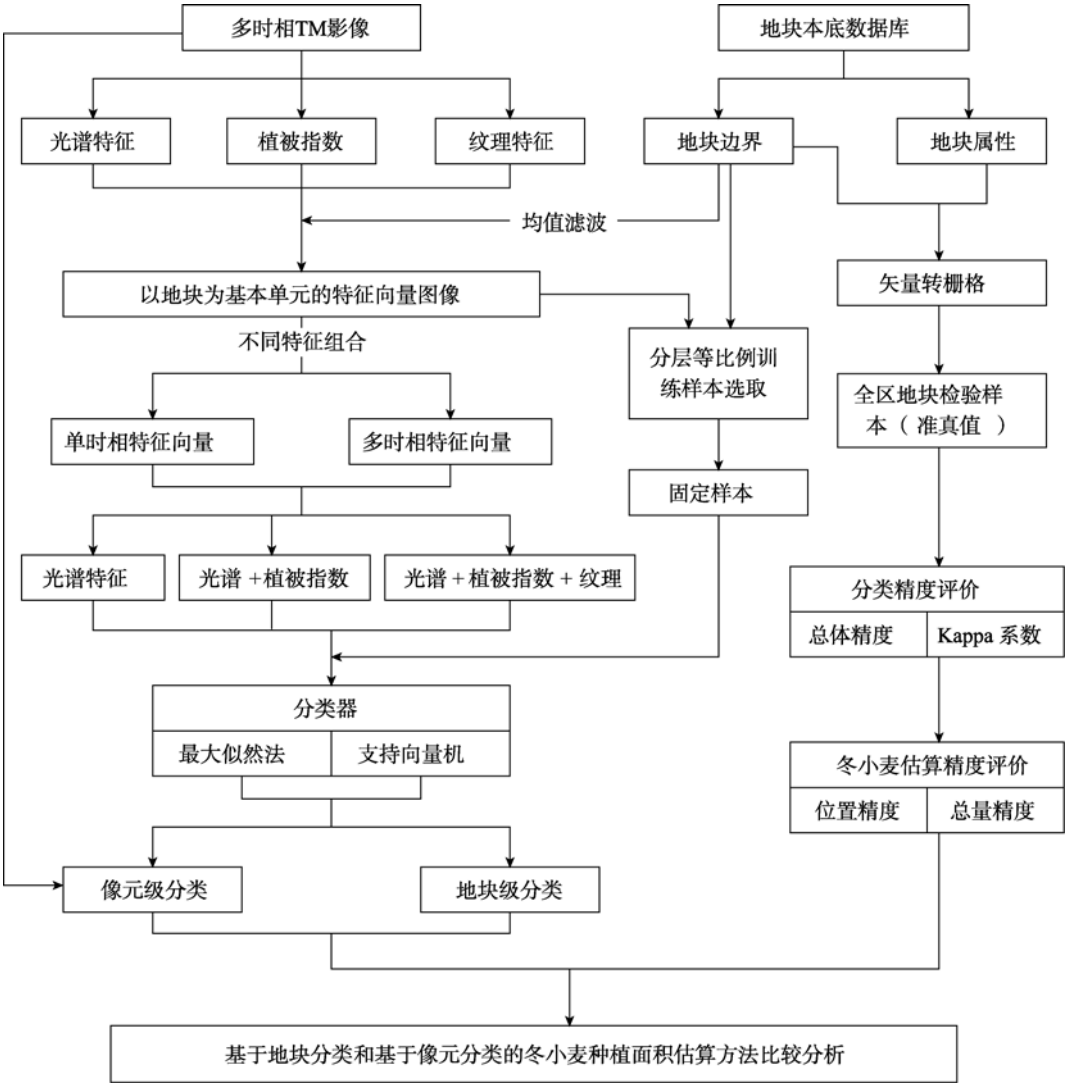

图 2 总体技术流程

3.1 地块变异系数计算

地块内是单一地物则为纯地块，地块内由多种地物组成则为混合地块，本研究暂对纯地块开展地块分类方法研究，而对于混合地块则将在后续的研究中开展混合地块分解方法研究。

耕地地块边界具有长期稳定性，可以通过历史高分辨率影像人工数字化获得，其地块内种植属性则年际变化较大，必须由现势中分辨率影像提供地块属性信息。由于耕地地块面积远大于 TM 像元大小，本研究以地块为基本单元，通过计算地块内的像元值变异系数来提取纯地块。变异系数(CV)，也称相对标准偏差(RSD)，其计算公式如下:

$$\mathrm{CV}=\frac{\sqrt{\dfrac{\sum(X_i-\bar{X})^2}{n}}}{\bar{X}} \tag{1}$$

式中，$\bar{X}$ 表示某个地块内的所有像元的某种特征向量的算术平均值；n 表示该地块边界内的像元个数；X_i 表示地块内某个像元的某种特征信息的像元值。

地块变异系数反映了耕地地块内部像元值的离散程度，变异系数越高，地块内混杂程度越大，反之则代表地块越纯，由于地块内同一作物仍会存在一定的变异，因此地块变异系数不可能达到 0。本文采用 3 个时相 TM 影像的 1—5、7 波段反射率进行地块变异系数计算，并采用野外数据对变异系数与实测样本地块的纯度进行对比验证。当 3 个时相 TM 的地块变异系数均小于 0.1，耕地地块为单一地物，反之则有两种或两种以上地物，因此本研究以地块变异系数 0.1 为阈值来区分实验区的纯地块和混合地块，见图 3。

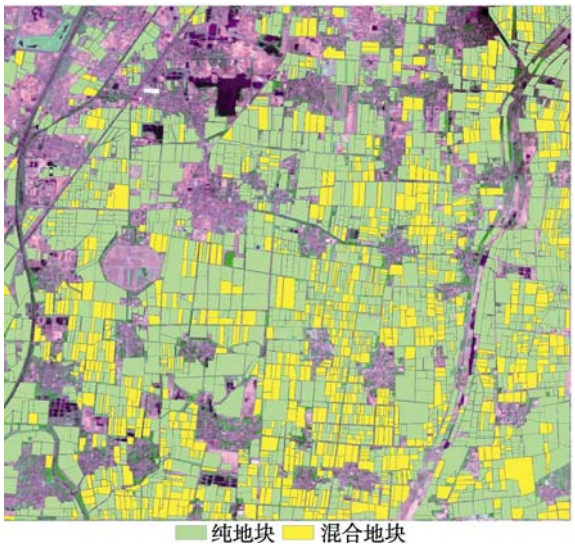

图 3 实验区纯地块与混合地块空间分布

3.2 分类器选择

现有遥感分类方法主要集中在利用遥感影像的波谱信息，采用距离、角度、概率等聚类准则或神经网络分类方法(陈亮等, 2007)。基于参数化密度分布函数判别的最大似然法(maximum likehood classification, MLC)是遥感影像监督分类最常用的方法(Richards & Jia, 1999; El-Magd & Tanton, 2003)。支持向量机(support vector machine, SVM)是近年来在影像分类、目标检测、数据融合等方面得到广泛应用的新型算法(何德平等, 2006; 何灵敏等, 2007)。

最大似然法与其他非参数方法相比具有易于与先验知识融合、算法简单、易于实施等优点，采用经验风险最小化准则，其前提是要有足够的训练样本。支持向量机是建立在统计学习理论的 VC 维理论和结构风险最小原理基础上的，根据有限的样本信息在模型的复杂性(即对特定训练样本的学习精度)和学习能力(即无错误地识别任意样本的能力)之间寻求最佳折衷，以期获得最好的推广能力(Drezetp & Harrison,2001)。

本文以冬小麦种植面积测量为目的，选用最大似然法和支持向量机两种代表性分类器，对不同特征向量组合进行基于地块和基于像元的分类方法对比研究。

3.3 特征向量组合方式

为了充分利用多时相 TM 影像的光谱特征、植被指数和纹理等特征向量信息，本文设计三层次特征向量组合方式分别进行地块分类研究(表 1)，其中光谱特征为 TM 影像的 6 个波段反射率，植被指数特征向量为 NDVI, RVI, SAVI, GVI, PVI, RDVI 共 6 种，纹理特征为各个时相 TM 影像第一主成分的角二阶距、相异性、熵、灰度相关 4 种纹理特征信息。

3.4 基于地块的特征向量提取

基于地块单元的特征向量信息提取的主要过程是：以像元为单元获取影像的各种特征向量，包括光谱反射率、植被指数、纹理等信息，按照地块边界与影像的空间位置关系，统计计算地块边界内的所有像元特征信息的平均值，将均值赋给地块内所有像元，使得基于地块单元的特征向量图像在所有地块内部的特征值是一致的。基于地块的特征向量信息提取公式如下:

$$F=\bar{X}=\frac{1}{n}\sum_{i=1}^{n}X_i \tag{2}$$

表 1 光谱、植被指数和纹理的三层次特征向量组合方式

层次	编号	特征向量组合方式
光谱	a	2006-12-03 TM 影像的 1—5、7 波段的反射率组合
	b	2007-04-26 TM 影像的 1—5、7 波段的反射率组合
	c	2007-05-28 TM 影像的 1—5、7 波段的反射率组合
	d	三时相 TM 影像的 1—5、7 波段的反射率组合
光谱+植被指数	e	2006-12-03 TM 影像的 6 种反射率与 6 种植被指数组合
	f	2007-04-26 TM 影像的 6 种反射率与 6 种植被指数组合
	g	2007-05 28 TM 影像的 6 种反射率与 6 种植被指数组合
	h	三时相 TM 影像的 6 种反射率和 6 种植被指数组合
光谱+植被指数+纹理	i	2006-12-03 TM 影像 6 种反射率、6 种植被指数和 4 种纹理组合
	j	2007-04-26 TM 影像 6 种反射率、6 种植被指数和 4 种纹理组合
	k	2007-05-28 TM 影像 6 种反射率、6 种植被指数和 4 种纹理组合
	l	三时相 TM 影像 6 种反射率、6 种植被指数和 4 种纹理组合

式中，$\bar{X}$ 表示某个地块内的所有像元的某种特征信息的算术平均值; n 表示该地块边界内的像元个数; X_i 表示该地块内某个像元的某种特征信息的像元值。

3.5 训练样本选取

为了确保训练样本真实地反映实验区的种植结构，尽可能地优化训练样本数量和质量，本研究采用分层等比例方式从地块数据库中随机选取训练样本，若在实际应用中则可通过野外调查数据来提供训练样本。其计算公式如下:

$$S=\sum_{i=1}^{n} N_i \times a\% \tag{3}$$

式中，S 为实验区选取的训练样本总量; n 为实验区的土地利用类型种类; N_i 为第 i 类土地利用类型地块的面积总量，由地块数据库提供先验知识; a%为每种土地利用类型的样本比例。

本研究对最大似然法和支持向量机进行多次实验，在保证分类精度稳定不变的前提下考虑计算速度，确定各个分类器的最优样本比例，其中最大似然法的训练样本比例定为 5%，SVM 对于小样本有着较优的学习能力，因此 SVM 分类的训练样本比例定为 1%。

3.6 精度评价体系构建

分类精度是指一幅不知道其质量的图像和一幅假设正确的图像(参考图)之间的吻合度。本研究以 QuickBird 影像目视解译的地块属性信息作为准真值，对多时相 TM 影像的地块级分类和像元级分类进行精度评价。由于本研究立足于通过分类方法、特征向量组合的对比分析，提高冬小麦种植面积估算的准确性，因此拟从影像分类精度和冬小麦种植面积估测精度两个方面构建精度评价体系。

3.6.1 影像分类精度

遥感影像分类精度最常用的评价方法是建立混淆矩阵，以此计算各种统计量并进行统计检验，最终给出对于总体和基于各种地物类型的分类精度值。本研究采用混淆矩阵、总体分类精度、Kappa 系数分别对各种特征向量组合的地块分类和像元分类结果进行精度评价。

3.6.2 冬小麦种植面积估算精度

本研究以 QuickBird 影像目视解译的冬小麦种植面积数据为准真值，从位置精度与面积总量精度两个方面，评价基于地块分类和像元分类的冬小麦种植面积估算的准确性。

(1) 位置精度

位置识别精度，是指实验区内所有地块或像元识别正确的百分比，这是遥感精度评价通常提供的指标，常常是研究者比较关心的精度指标。对于地块分类，本研究对冬小麦种植面积估算的位置精度以地块为单元进行评价; 对于像元分类，相应地以像元为单元进行评价。位置精度等同于冬小麦估算的产品精度，其计算公式为:

$$K_p=\frac{\sum P_i \times A_i}{A_0}\times 100\% \tag{4}$$

式中，P_i 表示某种特征向量组合的冬小麦识别结果与准真值相同的地块或像元; A_i 表示识别正确的地块面积或像元面积; A_0 表示从地块本底数据库中获取的冬小麦总面积准真值。

(2) 总量精度

区域总量精度描述的是一定范围的行政或自然单元内冬小麦种植面积总量与准真值总量的对比精度，这一指标是政府部门更关心的指标。总量精度的计算公式为:

$$K_r=1-\frac{|A_i-A_0|}{A_0}\times 100\% \tag{5}$$

式中，A_i 表示某种特征向量组合的基于地块分类或基于像元分类的整个区域冬小麦种植面积总量; A_0

表示 QuickBird 影像解译的冬小麦种植面积总量准真值。

4 结果分析

本文以高分辨率地块目视解译数据为准真值，采取地块变异系数来提取纯地块，分别以地块和像元为基本分类单元，提取多时相 TM 影像的光谱反射率、植被指数、纹理等特征向量，进行 3 个层次特征向量组合的地块级分类和像元级分类，从影像分类精度和冬小麦识别精度两方面进行精度评价。为了保证精度评价不依赖于某次随机值，本研究对每种特征向量组合进行 10 次样本选取与分类，并对平均精度进行评价分析。图 4 为实验区光谱+植被指数+纹理特征组合的最大似然、支持向量机的地块分类和像元分类结果图。

通过对比分析两种分类器的不同特征向量组合的影像分类精度和冬小麦种植面积估算精度，见图 5 与图 6，可得出以下结论。

4.1 分类单元分析

地块分类的影像分类精度和冬小麦识别精度均高于像元分类。地块分类在大多数特征向量组合上比像元分类的总体精度高 10%以上，Kappa 系数高出 0.1 以上。基于地块分类的冬小麦种植面积总量精度可达 95%，位置精度可达 90%，这是由于地块分类有效地降低了其他地类被错分为冬小麦的概率。说明以地块为基本单元的冬小麦分类即使在种植结构复杂的都市农业区，错分和漏分的概率远低于像元分类，由此可推断基于地块分类的冬小麦种植面积估算方法有着较好的区域适用能力。

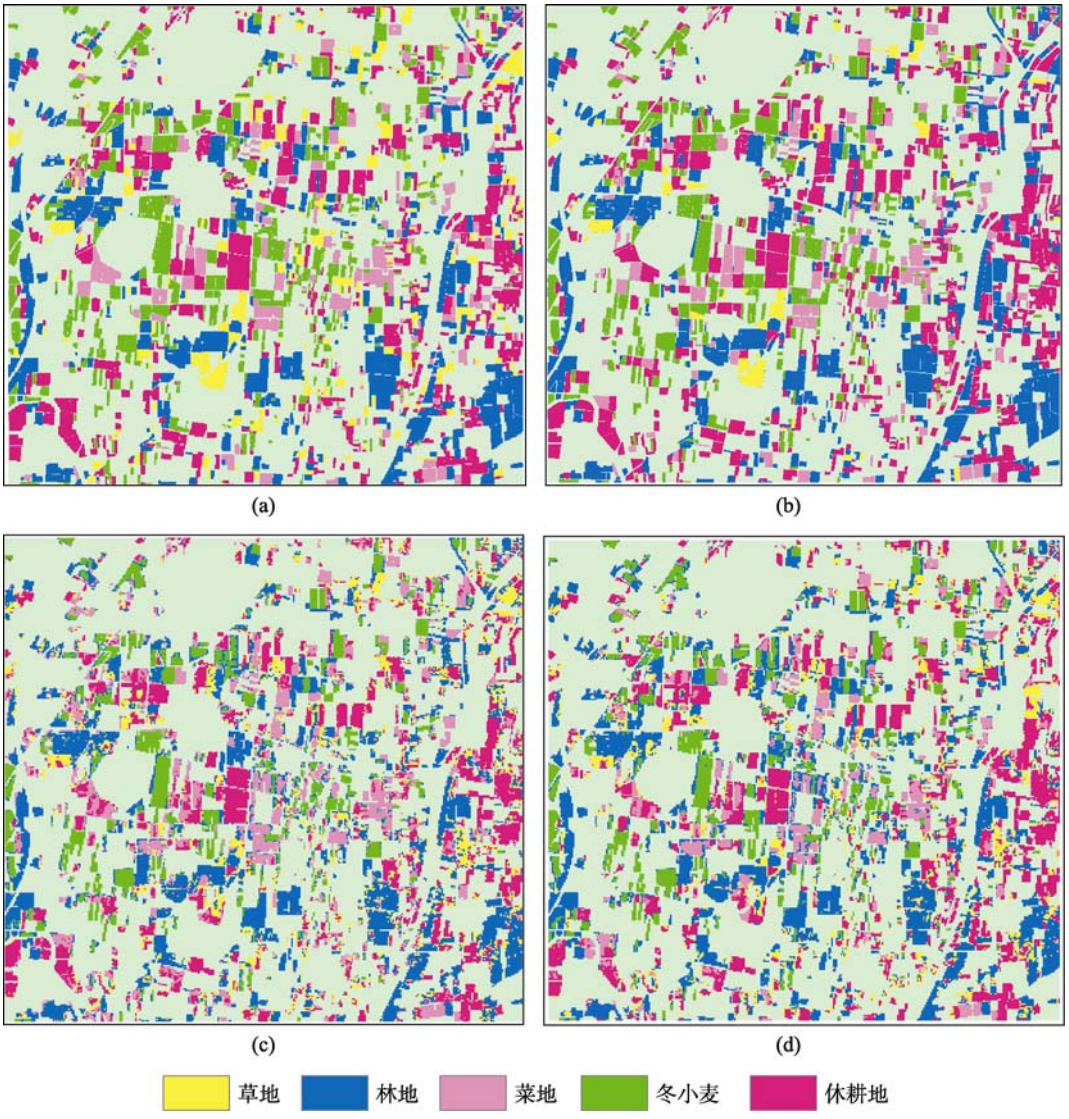

图 4 实验区光谱+植被指数+纹理特征组合的最大似然、支持向量机的地块分类和像元分类结果图
(a) MLC 地块分类; (b) SVM 地块分类; (c) MLC 像元分类; (d) SVM 像元分类

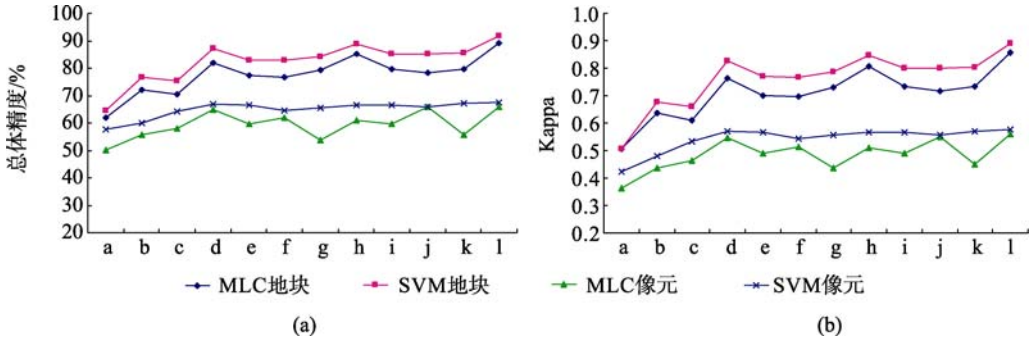

图 5　最大似然与支持向量机地块级、像元级分类总体精度与 Kappa 系数分析图
(横坐标 a, b, c, d, e, f, g, h, i, j, k, l 含义见表 1)
(a) 总体精度分析; (b) Kappa 系数分析

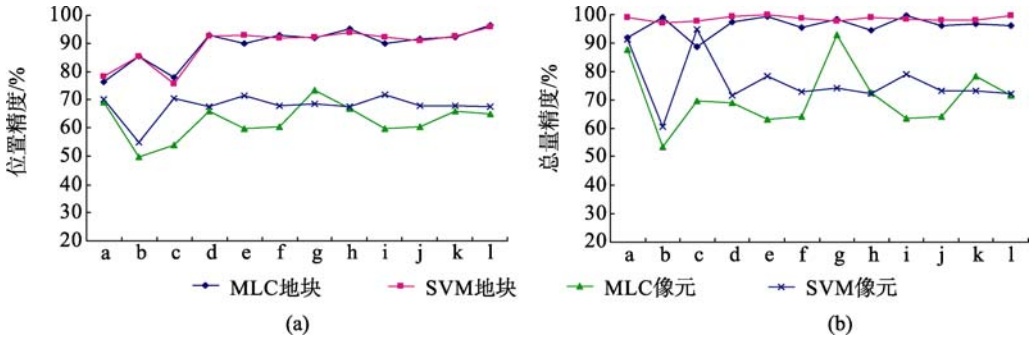

图 6　地块分类与像元分类的冬小麦种植面积总量精度与位置精度分析图
(横坐标 a, b, c, d, e, f, g, h, i, j, k, l 含义见表 1)
(a) 位置精度分析; (b) 总体精度分析

4.2　特征向量分析

随着特征向量的增加，地块分类的总体精度和 Kappa 系数的上升幅度高于像元分类，说明植被指数和纹理特征信息的加入，有助于提高地块分类的精度，但对于像元分类收效甚微。对于冬小麦种植面积估算，引入植被指数和纹理信息在一定程度上有助于提高地块分类的位置精度，但不会再提高冬小麦种植面积的总量精度。

4.3　TM 影像时相分析

多时相 TM 影像的地块分类精度高于单时相影像，说明作物物候差异有助于提高地块分类的总体精度和 Kappa 系数。随着 TM 影像的时相增多，冬小麦总量精度稳定不变，位置精度稳中有升，说明冬小麦特有的物候特征虽然不会明显提高种植面积总量精度，但有助于提高冬小麦地块的位置精度。从单时相影像的地块分类看，冬小麦拔节期的种植面积总量精度和位置精度高于越冬期和灌浆期。

为进一步分析冬小麦地块分类结果的误差来源，本文将地块按面积大小进行划分为不同等级区间，制定合适的 10 个面积区间，确保每个区间的地块数量接近一致，以精度较高的三时相光谱+植被指数+纹理的特征向量组合为例，对最大似然和 SVM 地块分类结果进行逐地块分析，提取分类正确地块、错分地块、漏分地块空间分布状况，统计分析不同面积区间的冬小麦地块分类的产品精度(正确率)、错分率和漏分率。

从图 7 可看出，冬小麦地块分类正确率(产品精度)随着地块面积的增大而递增，漏分率均随着地块面积的增大而递减；冬小麦地块分类的错分率随着地块面积的增大而呈波动式递减，在所有地块面积区间，最大似然的对冬小麦地块的错分率均高于 SVM，这是由于细碎地块容易产生光谱变异和光谱混淆，导致其他类型的细碎地块被错分为冬小麦的概率较大，大地块被错分的概率较低。SVM 由于对于小样本有着较强的学习能力，在样本量远少于最大似然的情况下，仍能得到较低的冬小麦地块错分率，因此 SVM 分类法相对于最大似然法更适用于冬小麦地块分类。

由于地块分类的冬小麦错分与漏分情况大多发生在破碎地块，其面积较小，对冬小麦种植面积总量的误差贡献也较小，而大地块发生错分与漏分情

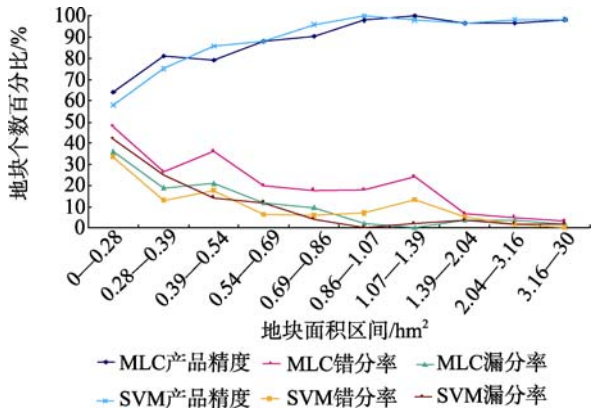

图 7 不同地块面积区间的冬小麦地块分类精度分析图

况较少，因此地块分类在整个区域能得到较高的位置精度和面积总量精度。对于少量的大面积冬小麦地块的错分与漏分，则可通过较小工作量的野外实地调查加以修正。

5 结论与讨论

本文选取种植结构复杂的都市农业区为方法实验区，以冬小麦种植面积估算为目标，通过高分辨率影像人工数字化的方式获取耕地地块边界，以地块为基本单元获取多时相 TM 影像特征信息，进行地块级和像元级分类对比分析，得出以下结论：基于地块分类的冬小麦种植面积估算方法相对于像元分类，有着较高的总量精度和位置精度，支持向量机与最大似然均能得到高达 97%的面积总量精度和 90%的位置精度；支持向量机的地块分类稳定性优于最大似然法，其所需的训练样本量远低于最大似然，因此支持向量机更加适用于冬小麦地块分类；植被指数和纹理信息有助于提高地块分类精度；采用地块分类提取冬小麦种植面积对 TM 影像的时相要求不高，在冬小麦拔节期能得到较高精度的冬小麦种植面积总量精度和位置精度；地块分类错分与漏分主要发生在细碎地块。

基于地块的作物分类的基本思想是以地块边界将中分辨率现势遥感影像分割成许多基本地块单元，使得地块内的所有像元作为整体参与分类处理。该方法充分利用了像元空间上下文，克服了由地块内部的光谱变异所引起的错分类问题，同时边界矢量数据能使得影像上的地块能与地面实际地块相对应，能对地块的空间位置、几何形状和景观特征实现正确表达，因而面向地块的分类法能有效地解决地块内部光谱变异和地块交界光谱混合的问题，即像元分类常见的“椒盐”现象。由于耕地地块边界具有长期稳定性，因此只需通过历史高分辨率影像数字化方式获取地块边界数据，实际上随着高分辨率影像获取能力的提高和国土“二调”成果的推广应用，耕地地块边界将会更为容易获取。而由于耕地地块的种植属性年际变化较大，判断地块是否纯地块和用于地块分类的特征向量信息则可以依赖于现势中分辨率影像，耕地地块实际面积远大于中分辨率像元面积，可以通过计算地块内像元值的变异系数来区分地块属于纯地块还是混合地块，对于纯地块则进行地块分类，而对于混合地块则将在后续的研究中开展混合地块分解方法研究。此外，以地块为基本单元的作物识别结果也有利于开展面向地块的变量水肥管理、病虫害防治、作物估产等工作。

一般认为，在种植结构单一、地块连片区域冬小麦较易识别，而地块破碎区域由于地块内部光谱变异和地块边界光谱混合较为严重而识别精度较低。本文选取的实验区是种植地块比较破碎的都市农业区，能得到较高的冬小麦种植面积估测精度，而对于种植结构单一区域理应得到更高的识别精度。因此，基于地块分类的冬小麦种植面积遥感估算方法的区域适应性较高，只要有比较准确的耕地地块边界数据，同时获取冬小麦关键生育期的单时相或多时相中分辨率现势影像，通过纯地块分类和混合地块分解相结合，就能准确地估算区域内的冬小麦种植面积。

本文在以下几个方面还需要在今后的研究中进一步补充：(1) 本文在 100km^2 的实验区进行地块分类方法研究，冬小麦种植规模较小，研究结果有待于在更大范围和不同种植结构的实验区内进行验证；(2) 实验区各地物类别的可分性直接影响分类精度，在本研究的冬小麦、休耕地、林地、草地和菜地的分类体系中，菜地与草地分类精度较低，这是由于实验区这两种地物分布较少，且在 12 月份易与休耕地产生特征混淆，但对冬小麦种植面积估算精度影响较小，若能在今后的研究中建立更为合理的分类体系，有望进一步提高地块分类精度。

REFERENCES

Aplin P, Atkinson P M and Curran P J. 1999. Fine spatial resolution simulated satellite sensor imagery for land cover mapping in the United Kingdom. *Remote Sensing of Environment*, **68**: 206—216

Banair A, Morin D, Bonn F and Huete A R. 1995. A review of vegetation Indices. *Remote Sens. Review*, **13**: 95—120

Chen C X, Yan T L and Zhu D H. 2001. The method of polygon land use identify supported by GIS. *Journal of China Agricul-*

tural University, **6**(3): 55—59

Chen L, Liu X and Zhang Y. 2007. A study of image classification based on MLC combined with spectral angle. *Engineering of Surveying and Mapping*, **16**(3): 40—47

Chen S S, Liu Q H, Chen L F, Li J and Liu Q. 2005. Review of research advances in remote sensing monitoring of grain crop area. *Transactions of the Chinese Society of Agricultural Engineering*, **21**(6): 166—171

David B.Lobell and Gregory P.Asner. 2004. Cropland distribution from temporal unmixing of MODIS data. *Remote Sensing of Environment*. **93**: 412—422

Drezetp M L and Harrison R F. 2001. A new method for sparsity control in support vector classification and regression. *Pattern Recogition*, **34**: 1112—1125

El-Magd I A and Tanton T W. 2003. Improvements in land Use mapping for irrigated agriculture from satellite sensor data using a multi stage maximum likelihood classification. *International Journal of Remote Sensing*, **24**(21): 4197—4206

Gu X H, Pan Y Z, Zhu X F, Zhang J S, Han L J and Wang S. 2007. Consistency study between MODIS and TM on winter wheat plant area monitoring. *Journal of Remote Sensing*, **11**(3): 350—358

He D P, Xiao Y, Xiao X G, Huang Y H and Zhou Q R. 2006. Application of the support vector machine in remote sensed image processing. *Urban Geotechnical Investigation & Surveying*, **3**: 27—30

He L M, Shen Z Q, Kong F S and Liu Z K. 2007. Study on multi-source remote sensing images classification with SVM. *Journal of Image and Graphics*, **12**(4): 648—654

Janssen L L F, Jaarsma M N and Van der Linden E T M. 1990. Integration topographic data with remote sensing for land-cover classification. Photogrammetric Engineering and Remote Sensing, **56**: 1503—1506

Langley S K, Cheshire H M and Humes K S. 2001. A comparison of single date and multitemporal satellite image classification in a semi-arid grassland. *Journal of Arid Environments*, **49**: 401—411

Liu J G, Zhang B, Zheng L F and Tong Q X. 2000. Urban remote sensing application study using hyperspectal data. *Journal of Remote Sensing*, **4**(3): 224—227

Lobo A, Chic O and Casterad A. 1996. Classification of mediterranean crops with multisensor data: per-pixel versus per-object statistics and image segmentation. *International Journal of Remote Sensing*, **17**: 2385—2400

Pedley M I and Curran P J. 1991. Per-field classification: an example using SPOT-HRV imagery. *International Journal of Remote Sensing*, **12**: 2181—2192

Shandley J, Franklin J and White T. 1996. Testing the Woodcock-Harward image segmentation algorithm in an area of southern California chaparral and woodland vegetation. *International Journal of Remote Sensing*, **17**: 983—1004

Smith G M and Fuller R M. 2001. An integrated approach to land cover classification: an example in the Island of Jersey. *International Journal of Remote Sensing*, **22**: 3123—3142

Smith G M and Fuller R M. 2001. An integrated approach to land cover classification: an example in the Island of Jersey. *International Journal of Remote Sensing*, **22**: 3123—3142

Van Niel, T G. and McVicar, T R. 2003. A simple method to improve field-level rice identification: toward operational monitoring with satellite remote sensing. *Australian Journal of Experimental Agriculture*, **43**: 379—387

Wu J P, Mao Z H, Chen J Y and Pan D L. 2006. A new classification method for coast remote sensing image. *Journal of Martine Sciences*, **24**(2): 70—78

附中文参考文献

陈亮, 刘希, 张元. 2007. 结合光谱角的最大似然法遥感影像分类. 测绘工程, **16**(3): 40—47

陈水森, 柳钦火, 陈良富, 李静, 刘强. 2005. 粮食作物播种面积遥感监测研究进展. 农业工程学报. **21**(6): 66—170

程昌秀, 严泰来, 朱德海. 2001. GIS 辅助下的图斑地类识别方法研究——以土地利用动态监测为例. 中国农业大学学报, **6**(3): 55—59

顾晓鹤, 潘耀忠, 朱秀芳, 张锦水, 韩立建, 王双. 2007. MODIS 与 TM 冬小麦种植面积遥感测量一致性研究. 遥感学报, **11**(3): 350—358

何德平, 肖勇, 肖兴国, 黄永红, 周庆人. 2006. 支持向量机在遥感影像处理中的应用. 城市勘测, 3: 27—30

何灵敏, 沈掌泉, 孔繁胜, 刘震科. 2007. SVM 在多源遥感图像分类中的应用研究. 中国图象图形学报, **12**(4): 648—654

刘建贵, 张兵, 郑兰芬, 童庆禧. 2000. 成像光谱数据在城市遥感中的应用研究. 遥感学报, **4**(3): 224—227

吴均平, 毛志华, 陈建裕, 潘德炉. 2006. 一种基于分割图斑的海岸带遥感图像分类方法. 海洋学研究, **24**(2): 70—78